J Surg Med. 2022;6(1):68-71.
DOI: 10.28982/josam.990310

Research article

Journal of Surgery and Medicine
e-ISSN=2602-2079

MRI histogram analysis of optic nerves in children with type 1 neurofibromatosis

Yeşim Eroğlu, Murat Baykara

Firat University, Faculty of Medicine, Department of Radiology, Elazig, Turkey

ORCID ID of the author(s)
YE: 0000-0003-3636-4810
MB: 0000-0003-2588-9013

Corresponding Author
Yeşim Eroğlu
Firat University, Faculty of Medicine, Department of Radiology, Elazig, Turkey
E-mail: dryesimeroglu@gmail.com

Ethics Committee Approval
The study was approved by the Ethics Committee of Fırat University (Issue: E-97132852-050.01.04-49705; Date: 03.06.2021).
All procedures in this study involving human participants were performed in accordance with the 1964 Helsinki Declaration and its later amendments.

Conflict of Interest
No conflict of interest was declared by the authors.

Financial Disclosure
The authors declared that this study has received no financial support.

Published
2022 January 25

Abstract

Background/Aim: Type 1 neurofibromatosis (NF1) is the most common neurocutaneous disease affecting numerous systems. Optic pathway glioma (OPG) is a common tumor in children with NF1 and often has variable clinical presentations. In this study, histogram analysis parameters of optic nerves were measured in the magnetic resonance images (MRI) of children with NF1 and compared with a control group.
Methods: This case-control study consisted of three groups: Ten patients with NF1 without optic pathway glioma (bilateral optic nerve, n: 20), four patients with NF1 with bilateral optic pathway glioma (n: 8), and nineteen healthy controls (n: 38). ROIs were placed on bilateral pre-chiasmatic optic nerves in the images. With histogram analysis, average gray level intensity (mean), the standard deviation, minimum, median, and maximum intensity, uniformity, entropy, kurtosis, variance, skewness, size% M, size% U, size% L, and percentiles were measured.
Results: Mean, median, 3%, 5%, 10%, 25%, and 75% values were higher in NF1 patients with optic pathway glioma (NF1-OPG) than in NF1 patients without optic pathway glioma (NF1-woOPG), and the control group (P<0.001). The same values were significantly higher in the NF1-woOPG group compared to the control group (P<0.001). The minimum, maximum, 1%, 90%, 95%, 97%, and 99% values were significantly higher in the NF1-OPG and NF1-woOPG groups than the control group (P<0.001). The entropy value was significantly higher in the NF1-OPG group than the NF1-woOPG and control groups (5.73, 4.93, and 5.25, respectively, P=0.016).
Conclusion: MRI histogram analysis revealed significant differences between NF1-OPG, NF1-woOPG, and healthy individuals in terms of optic nerves. Thus, we think that it can be used to monitor the optic nerves of children with NF1.

Keywords: Type 1 Neurofibromatosis, Image processing, Magnetic resonance imaging, Optic nerve

How to cite: Eroğlu Y, Baykara M. MRI histogram analysis of optic nerves in children with type 1 neurofibromatosis. J Surg Med. 2022;6(1):68-71.

Introduction

Type 1 neurofibromatosis (NF1) is the most common neurocutaneous disease affecting numerous organs. Its prevalence is approximately 1/2500-3000 [1]. Patients with NF1 are predisposed to tumor development, especially in the central nervous system. Pilocytic astrocytoma with low mitotic activity is the most common tumor. These tumors most occur in the optic pathway [2]. Although optic pathway gliomas tend to grow slowly and are mostly benign, their clinical progression varies greatly. The prevalence of OPG in children with NF1 is approximately 15-20%. Almost 30-50% of them become symptomatic and progressive vision loss occurs [3]. Patients are evaluated with intermittent ophthalmic examinations. There may be difficulties in evaluating the visual acuity of young children. Treatments such as chemotherapy, radiotherapy, and surgery are used in patients with reduced visual acuity. Therefore, markers are needed to predict the likely changes in the optic nerves. Imaging findings are not sufficient to evaluate the microscopic and macroscopic structure of the optical pathways or to predict the clinical course [4]. The determination of the microstructural changes of the optic nerves in NF1 may contribute to the estimation of the clinical course in these children and determine follow-up and treatment.

Histogram analysis, one of the texture analysis methods, is widely used for tumor characterization, determination of normal and abnormal tissues, guiding radiotherapy, diagnosing interstitial lung disease, and deciding various prognostic factors [5-9]. The digital medical images consist of units called pixels. Each pixel contains a quantitative value of the gray level density that forms the basis of the image. Histogram analysis enables the calculation of the grayscale levels of all pixels in the region of interest (ROI). Thus, it provides a more detailed evaluation of the structure of tissues compared to the human eye [10].

In this study, we compared the histogram analysis parameters of the optic nerves in the MRIs of children with NF1 with a control group.

Materials and methods

Study population

Approval for this case-control study was obtained from the non-interventional research ethics committee of our university (Date: 27.05.2021, Decision number: 2021/07-22). All pediatric patients diagnosed with NF1 according to the diagnostic criteria whose brain MRIs were performed in our hospital between January 2015 and February 2021 were analyzed [11]. Patients whose brain MRI was performed with a different device and with a different protocol were excluded from the study. Finally, fourteen children (4 patients with bilateral optic glioma) with NF1 were included. Nineteen age- and gender-matching healthy controls with normal visual acuity and neurological examination, and no pathological findings in the brain MRI comprised the control group. The study consisted of three groups: NF1-woOPG, NF1-OPG, and control.

Image acquisition

A 3 Tesla (T) scanner was used to obtain the MRI scans of the patients (Philips, Ingenia, Netherlands, 3T). T2-weighted images were obtained in the coronal plane (Repetition time: 2500 ms, time echo: 260 ms, slice thickness: 1 mm, spacing between slices: 0.5 mm).

Image analysis

The histogram yields information about pixels, which are small units of the image [10]. This information contains the mean gray level intensity (mean), median, standard deviation of the histogram, minimum and maximum intensity values, uniformity, kurtosis, entropy, skewness, variance, size %mean, size %upper, size %lower (size% M, size% U, size% L) and percentiles [12-14]. Entropy shows the inhomogeneity of gray level density within the ROI [15]. Uniformity shows the uniform distribution of gray tones in the measured area [16]. Skewness expresses the asymmetry in the distribution of gray tones [16]. Kurtosis is the peak value of the distribution [16].

Images were transmitted to an iMac computer (Apple Inc., 27-inch, Cupertino, CA, USA). Horos Open-Source Medical Image Viewer V.3.3.6 imaging software (Nimble Co LLC d/b/a Purview in Annapolis, MD, USA, and Horosproject.org) was used for histogram analysis in the ROI. An ROI was placed in the bilateral pre-chiasmatic optic nerves in coronal T2-weighted images without exceeding the boundaries (Figure 1).

Figure 1: Coronal T2-weighted MR image (a, b) showed ROI placement on the bilateral optic nerves of a patient with NF1-OPG

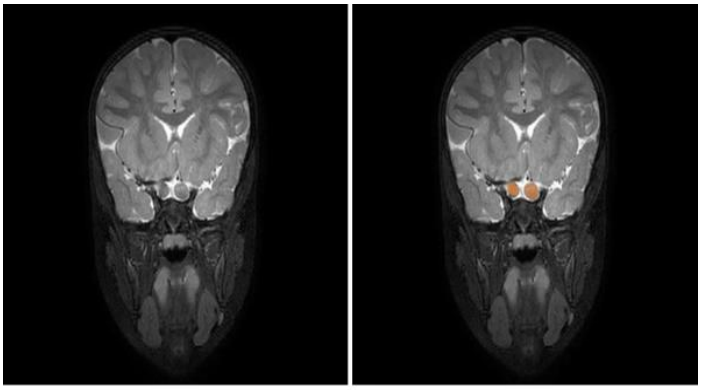

The mean gray level intensity, standard deviation, variance, uniformity, entropy, kurtosis, skewness, size% M, size% U, size% L, and percentiles were calculated in the ROI. A program written in MATLAB was used to analyze the images (version R2017a, Natick, MA, MathWorks, USA).

Statistical analysis

The data were expressed in mean (standard deviation). Statistical analysis was performed with the IBM SPSS 25 program. The Kolmogorov-Smirnov test was used to assess the normality of distribution. The Chi-Square test was used to compare the groups in terms of gender. ANOVA and Kruskal-Wallis tests were performed to compare other parameters. $P<0.05$ indicated statistical significance. Receiver-operating characteristic (ROC) analysis was performed to differentiate the significant values of the NF1-OPG group from the control and NF1-woOPG groups.

Results

There were 5 males and 5 females in the NF1-woOPG group, 4 males in the NF1-OPG group, and 12 males and 7 females in the control group. The mean ages of the control, NF1-woOPG, and NF1-OPG groups were 9.37 (4.04) years, 9.30 (3.76) years, and 8.00 (4.96) years, respectively (P=0.683).

The mean, median, 3%, 5%, 10%, 25%, and 75% values were significantly higher in the NF1-OPG group compared to the NF1-woOPG and the control groups, and in the NF1-woOPG group compared to the control group. The minimum, maximum, 1%, 90%, 95%, 97%, and 99% values were significantly higher in the NF1-OPG and NF1-woOPG groups compared to the control group, and similar between the NF1-OPG and the NF1-woOPG groups.

The entropy value was significantly higher in the NF1-OPG group compared to the NF1-woOPG group and the control group, and similar between the NF1-woOPG and the control groups. The other parameters were comparable (Table 1 and 2) (Figure 2).

Table 1: Histogram analysis of optic nerves according to the groups

	Control (38) Mean (SD)	NF1-woOPG (20) Mean (SD)	NF1-OPG (8) Mean (SD)	*P*-value
Age	9.37 (4.04)	9.30 (3.76)	8.00 (4.96)	0.683†
Mean	154.80 (33.20)	215.41 (54.26)	268.70 (87.22)	<0.001†
SD	43.90 (11.72)	54.50 (17.08)	48.14 (13.92)	0.125†
Minimum	81.05 (32.82)	129.40 (57.55)	166.25 (73.07)	<0.001†
Maximum	268.16 (67.95)	363.75 (87.54)	389.38 (63.32)	<0.001*
Median	149.28 (32.52)	210.58 (56.59)	267.13 (93.14)	<0.001†
Variance	2060.54 (1085.45)	3247.14 (2005.36)	2486.64 (1553.81)	0.125†
Entropy	5.25 (0.23)	4.93 (0.51)	5.73 (1.14)	0.016†
Size %L	14.36 (4.68)	14.31 (6.44)	16.16 (3.88)	0.651*
Size %U	15.42 (3.79)	15.66 (4.21)	15.79 (3.45)	0.958*
Size %M	70.22 (6.11)	70.02 (9.63)	68.05 (6.86)	0.752*
Kurtosis	3.32 (1.18)	4.05 (3.06)	3.25 (1.41)	0.588†
Skewness	0.57 (0.62)	0.78 (0.72)	0.18 (0.67)	0.101*
Uniformity	0.23 (0.07)	0.21 (0.09)	0.28 (0.13)	0.325†
1st percentile	81.19 (32.78)	129.45 (57.51)	178.40 (84.05)	<0.001†
3rd percentile	87.97 (31.39)	135.37 (54.88)	186.60 (87.39)	<0.001†
5th percentile	92.96 (30.98)	143.55 (51.42)	194.93 (83.77)	<0.001†
10th percentile	103.71 (31.37)	155.02 (47.76)	207.75 (86.11)	<0.001†
25th percentile	124.83 (31.54)	174.94 (47.63)	234.44 (93.30)	<0.001†
75th percentile	178.24 (35.99)	243.81 (58.03)	303.53 (86.76)	<0.001†
90th percentile	215.44 (44.12)	291.53 (69.05)	331.10 (84.11)	<0.001†
95th percentile	241.33 (57.35)	320.56 (80.21)	348.85 (79.61)	<0.001†
97th percentile	253.00 (63.35)	337.21 (87.62)	362.51 (76.62)	<0.001*
99th percentile	267.40 (67.07)	363.20 (87.63)	376.18 (69.92)	<0.001*

SD: Standard Deviation, * ANOVA Test, † Kruskal-Wallis Test

Table 2: Significantly differing parameters between the groups

	P-value*		
	Control versus NF1-woOPG	Control versus NF1-OPG	NF1-woOPG versus NF1-OPG
Mean	<0.001	<0.001	0.030
Minimum	0.001	<0.001	0.157
Maximum	<0.001	<0.001	0.687
Median	<0.001	<0.001	0.025
Entropy	0.064	0.044	0.001
1st percentile value	0.002	<0.001	0.052
3rd percentile value	0.002	<0.001	0.036
5th percentile value	0.001	<0.001	0.027
10th percentile value	<0.001	<0.001	0.021
25th percentile value	0.001	<0.001	0.010
75th percentile value	<0.001	<0.001	0.019
90th percentile value	<0.001	<0.001	0.241
95th percentile value	<0.001	<0.001	0.580
97th percentile value	<0.001	0.001	0.697
99th percentile value	<0.001	0.001	0.908

* Post Hoc Tukey HSD Test

Figure 2: (a) mean, (b) minimum, (c) maximum and (d) entropy value distributions of groups

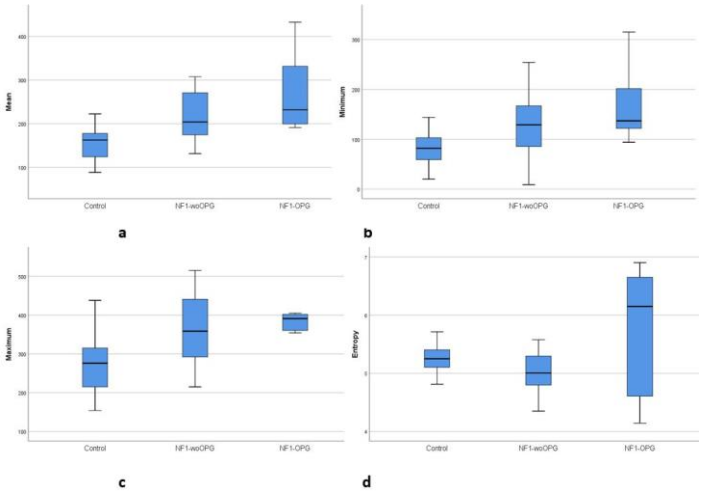

In the ROC analysis for mean value (Figure 3a), when AUC = 0.875 and the threshold=197.27, the NF1-OPG group could be distinguished from the NF1-woOPG and the control groups with 87.5% sensitivity and 77.6% specificity.

In the ROC analysis for minimum value (Figure 3b), when AUC = 0.809 and threshold=114.5, the NF1-OPG group could be distinguished from the NF1-woOPG and the control group with 87.5% sensitivity and 70.7% specificity.

In the ROC analysis for maximum value (Figure 3c), when AUC = 0.813 and threshold=363.5, the NF1-OPG group could be distinguished from the control and the NF1-woOPG groups with 75.0% sensitivity and 79.3% specificity.

In the ROC analysis for entropy value (Figure 3d), when AUC = 0.667 and threshold=5.77, the NF1-OPG group could be distinguished from the NF1-woOPG and the control groups with 62.5% sensitivity and 98.3% specificity.

Figure 3: (a) mean, (b) minimum, (c) maximum and (d) entropy value Receiver-Operating Characteristic (ROC) graphs for distinguishing the NF1-OPG group from the control and NF1-woOPG groups

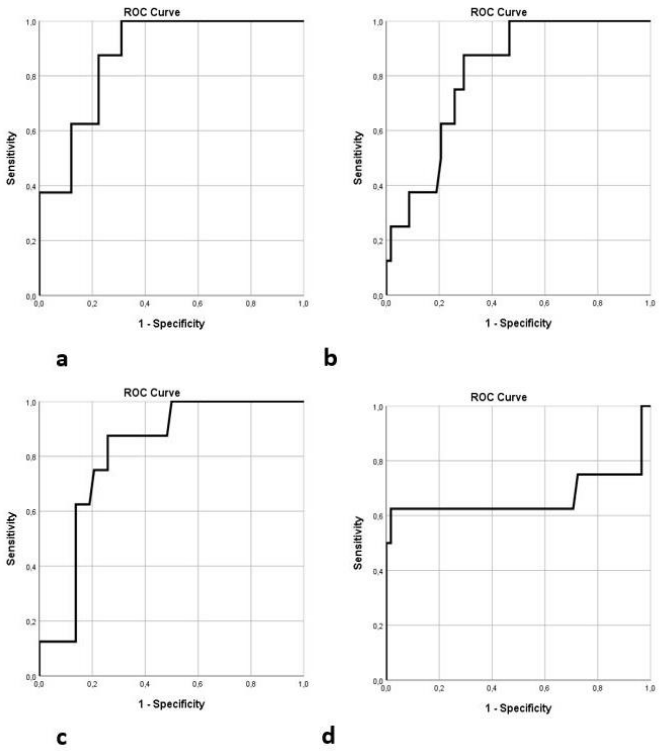

Discussion

Type 1 Neurofibromatosis is a neurocutaneous disease with high morbidity, affecting many organs and systems [17]. OPG is a common central nervous system tumor in children with NF1 [1]. The clinical course is variable. While some children may experience rapid tumor progression and vision loss, some present with regression despite similar neuroimaging findings. The imaging method primarily used in the diagnosis and follow-up of these tumors is MRI [18]. Neuroimaging findings are not sufficient to evaluate these tumors in terms of microstructural aspects [19, 20]. Prognostic factors are needed to predict the development of OPG and the possible clinical course in these children. A study conducted to evaluate the clinical course of children with OPG reported that the increased mean permeability values in dynamic contrast MRI may suggest aggressive OPG [4]. Another study performed with diffusion-weighted MRI in children with OPG stated that high apparent diffusion coefficient values may be related to the rapid progression of the tumor [21].

Histogram analysis is an increasingly popular method of texture analysis. It provides numerical acquisition of pixel-level differences in areas that the human eye cannot distinguish on images [22]. In the literature, histogram analysis has been used in the detection and classification of brain tumors in numerous diseases such as multiple sclerosis, acute ischemia, Alzheimer's, and tinnitus [23-27]. In a study on multiple sclerosis patients, histogram analysis showed a difference in the structure of the optic nerve compared to the controls [28]. In another study, a difference was found in histogram analysis parameters between the normal optic nerves and the enhanced and non-enhanced optic nerves in patients with optic neuritis [29]. We found significant differences between the optic nerves of the healthy controls and the NF1-woOPG and NF1-OPG children using MRI histogram analysis. In addition, the MRI histogram parameters in the optic nerves that were considered normal in conventional MRI in children with NF1 were found to differ from those of healthy individuals. This may contribute to the evaluation of normal optic nerves with MRI, especially in young children whose visual acuity cannot be measured clearly on ophthalmological examination.

Limitations

This is a retrospective study involving a small patient population. The number of patients with NF1-OPG was sparse. Also, there were not enough patients who underwent imaging with a more easily accessible MR device with a lower Tesla, so patients who underwent MRI with a 3T MR device were included for a more homogeneous analysis. To the best of our knowledge, no previous studies are evaluating the optic nerves of children with NF1 by MRI histogram analysis. We think that our study will be a guide for future studies with larger and homogeneous patient series.

Conclusion

There is a need for markers that will provide insight into the development and progression of OPG in children with NF1. Using MRI histogram analysis, we found significant differences between the optic chiasms of children with NF1-woOPG, NF1-OPG, and healthy children. We think that it is promising that the optic nerves of patients with NF1-woOPG, which appear normal in MRI studies, differ from the optic nerves of healthy individuals in histogram analysis. According to our study, MRI histogram analysis may be a viable option in evaluating optic nerve changes in NF1.

References

1. Campen CJ, Gutmann DH. Optic Pathway Gliomas in Neurofibromatosis Type 1. J Child Neurol. 2018;33(1):73-81. doi: 10.1177/0883073817739509.
2. Guillamo JS, Créange A, Kalifa C, Grill J, Rodriguez D, Doz F, et al. Prognostic factors of CNS tumours in Neurofibromatosis 1 (NF1): a retrospective study of 104 patients. Brain. 2003;126(Pt 1):152-60. doi: 10.1093/brain/awg016.
3. Binning MJ, Liu JK, Kestle JR, Brockmeyer DL, Walker ML. Optic pathway gliomas: a review. Neurosurg Focus. 2007;23(5):E2. doi: 10.3171/FOC-07/11/E2.
4. Jost SC, Ackerman JW, Garbow JR, Manwaring LP, Gutmann DH, McKinstry RC. Diffusion-weighted and dynamic contrast-enhanced imaging as markers of clinical behavior in children with optic pathway glioma. Pediatr Radiol. 2008;38(12):1293-9. doi: 10.1007/s00247-008-1003-x.
5. Aerts HJ, Bussink J, Oyen WJ, van Elmpt W, Folgering AM, Emans D, et al. Identification of residual metabolic-active areas within NSCLC tumours using a pre-radiotherapy FDG-PET-CT scan: a prospective validation. Lung Cancer. 2012;75(1):73-6. doi: 10.1016/j.lungcan.2011.06.003.
6. McLaren CE, Chen WP, Nie K, Su MY. Prediction of malignant breast lesions from MRI features: a comparison of artificial neural network and logistic regression techniques. Acad Radiol. 2009;16(7):842-51. doi: 10.1016/j.acra.2009.01.029.
7. Baykara M, Koca TT, Demirel A, Berk E. Magnetic resonance imaging evaluation of the median nerve using histogram analysis in carpal tunnel syndrome. Neurological Sciences and Neurophysiology. 2018;35(3):145-50. doi:10.5152/NSN.2018.11280.
8. Colombi D, Dinkel J, Weinheimer O, Obermayer B, Buzan T, Nabers D, et al. Visual vs Fully Automatic Histogram-Based Assessment of Idiopathic Pulmonary Fibrosis (IPF) Progression Using Sequential Multidetector Computed Tomography (MDCT). PLoS One. 2015;10(6):e0130653. doi: 10.1371/journal.pone.0130653.
9. Molina D, Pérez-Beteta J, Luque B, Arregui E, Calvo M, Borrás JM, et al. Tumour heterogeneity in glioblastoma assessed by MRI texture analysis: a potential marker of survival. Br J Radiol. 2016;89(1064):20160242. doi: 10.1259/bjr.20160242.
10. Castellano G, Bonilha L, Li LM, Cendes F. Texture analysis of medical images. Clin Radiol. 2004 Dec;59(12):1061-9. doi: 10.1016/j.crad.2004.07.008.
11. Raus I, Coroiu RE, Capusan CS. Neuroimaging in pediatric phakomatoses. An educational review. Clujul Med. 2016;89(1):56-64. doi: 10.15386/cjmed-417.
12. Baykara S, Baykara M, Mermi O, Yildirim H, Atmaca M. Magnetic resonance imaging histogram analysis of corpus callosum in a functional neurological disorder. Turk J Med Sci. 2021;51(1):140-7. doi: 10.3906/sag-2004-252.
13. Yildirim M, Baykara M. Differentiation of progressive disease from pseudoprogression using MRI histogram analysis in patients with treated glioblastoma. Acta Neurol Belg. 2021 Feb 8. doi: 10.1007/s13760-021-01607-3.
14. Yildirim M, Baykara M. Differentiation of Multiple Myeloma and Lytic Bone Metastases: Histogram Analysis. J Comput Assist Tomogr. 2020;44(6):953-5. doi: 10.1097/RCT.0000000000001086.
15. Ganeshan B, Miles KA, Young RC, Chatwin CR. Texture analysis in non-contrast enhanced CT: impact of malignancy on texture in apparently disease-free areas of the liver. Eur J Radiol. 2009;70(1):101-10. doi: 10.1016/j.ejrad.2007.12.005.
16. Ganeshan B, Panayiotou E, Burnand K, Dizdarevic S, Miles K. Tumour heterogeneity in non-small cell lung carcinoma assessed by CT texture analysis: a potential marker of survival. Eur Radiol. 2012;22(4):796-802. doi: 10.1007/s00330-011-2319-8.
17. Arslan A. Carotid intima-media thickness and cardiac functions in children with neurofibromatosis type 1. J Surg Med. 2019;3(7):525-7. doi: 10.28982/josam.595760.
18. Prada CE, Hufnagel RB, Hummel TR, Lovell AM, Hopkin RJ, Saal HM, et al. The Use of Magnetic Resonance Imaging Screening for Optic Pathway Gliomas in Children with Neurofibromatosis Type 1. J Pediatr. 2015;167(4):851-6.e1. doi: 10.1016/j.jpeds.2015.07.001.
19. Lambron J, Rakotonjanahary J, Loisel D, Frampas E, De Carli E, Delion M, et al. Can we improve accuracy and reliability of MRI interpretation in children with optic pathway glioma? Proposal for a reproducible imaging classification. Neuroradiology. 2016;58(2):197-208. doi: 10.1007/s00234-015-1612-7.
20. Zahavi A, Toledano H, Cohen R, Sella S, Luckman J, Michowiz S, et al. Use of Optical Coherence Tomography to Detect Retinal Nerve Fiber Loss in Children With Optic Pathway Glioma. Front Neurol. 2018;9:1102. doi: 10.3389/fneur.2018.01102.
21. Yeom KW, Lober RM, Andre JB, Fisher PG, Barnes PD, Edwards MS, et al. Prognostic role for diffusion-weighted imaging of pediatric optic pathway glioma. J Neurooncol. 2013;113(3):479-83. doi: 10.1007/s11060-013-1140-4.
22. Radulescu E, Ganeshan B, Shergill SS, Medford N, Chatwin C, Young RC, et al. Grey-matter texture abnormalities and reduced hippocampal volume are distinguishing features of schizophrenia. Psychiatry Res. 2014;223(3):179-86. doi: 10.1016/j.pscychresns.2014.05.014.
23. Won SY, Park YW, Park M, Ahn SS, Kim J, Lee SK. Quality Reporting of Radiomics Analysis in Mild Cognitive Impairment and Alzheimer's Disease: A Roadmap for Moving Forward. Korean J Radiol. 2020;21(12):1345-54. doi: 10.3348/kjr.2020.0715.
24. Chen Q, Xia T, Zhang M, Xia N, Liu J, Yang Y. Radiomics in Stroke Neuroimaging: Techniques, Applications, and Challenges. Aging Dis. 2021;12(1):143-54. doi: 10.14336/AD.2020.0421.
25. Kassner A, Thornhill RE. Texture analysis: a review of neurologic MR imaging applications. AJNR Am J Neuroradiol. 2010;31(5):809-16. doi: 10.3174/ajnr.A2061.
26. Chekouo T, Mohammed S, Rao A. A Bayesian 2D functional linear model for gray-level co-occurrence matrices in texture analysis of lower grade gliomas. Neuroimage Clin. 2020;28:102437. doi: 10.1016/j.nicl.2020.102437.
27. Baykara M, Sagiroglu S. An evaluation of magnetic resonance imaging with histogram analysis in patients with idiopathic subjective tinnitus. North Clin Istanb. 2018;6(1):59-63. doi: 10.14744/nci.2018.72593.
28. Dogan A, Baykara M. The evaluation of the optic nerve in multiple sclerosis using MRI histogram analysis. Ann Med Res. 2020;27(3):780-3.
29. Liu HJ, Zhou HF, Zong LX, Liu MQ, Wei SH, Chen ZY. MRI Histogram Texture Feature Analysis of the Optic Nerve in the Patients with Optic Neuritis. Chin Med Sci J. 2019;34(1):18-23. doi: 10.24920/003507.

This paper has been checked for language accuracy by JOSAM editors.
The National Library of Medicine (NLM) citation style guide has been used in this paper.